Journal of Physics G: Nuclear and Particle Physics

R-matrix analysis of the ^{3}He(n, p)^{3}H and ^{7}Be(n, p)^{7}Li reactions

INSTITUTE OF PHYSICS PUBLISHING JOURNAL OF PHYSICS G: NUCLEAR AND PARTICLE PHYSICS

J. Phys. G: Nucl. Part. Phys. **29** (2003) 395–403 PII: S0954-3899(03)55003-4

R-matrix analysis of the ^{3}He(n, p)^{3}H and ^{7}Be(n, p)^{7}Li reactions

Abderrahim Adahchour[1] **and Pierre Descouvemont**[2]

Physique Nucléaire Théorique et Physique Mathématique, CP229 Université Libre de Bruxelles, B1050 Brussels, Belgium

Received 21 October 2002
Published 20 January 2003
Online at stacks.iop.org/JPhysG/29/395

Abstract

We apply the *R*-matrix formalism to the ^{3}He(n, p)^{3}H and ^{7}Be(n, p)^{7}Li reactions, which play an important role in the big-bang nucleosynthesis. The cross sections are analysed along with the ^{4}He and ^{8}Be spectra near threshold. Neutron and proton widths of high-energy states are determined. A statistical analysis of the uncertainties provide fairly low error bars (typically 2% at the 1σ confidence level) on the reaction rates.

1. Introduction

The ^{3}He(n, p)^{3}H and ^{7}Be(n, p)^{7}Li reactions play an important role both in nuclear physics and in astrophysics [1–4]. In nuclear physics, they represent a good tool to investigate the ^{4}He and ^{8}Be spectra in the high-energy region (the thresholds are at 20.58 MeV and 18.90 MeV, respectively). On the other hand, both reactions are known to be quite important in the calculated abundances of ^{3}He and ^{7}Li in the primordial nucleosynthesis [5–8]. A recent experiment by Brune *et al* [9] aimed at improving previous data on ^{3}He(n, p)^{3}H [10–15] through the ^{3}H(p, n)^{3}He mirror reaction. Brune *et al* cover the energy range from $E_p = 1.02$ MeV to 4.50 MeV; they confirm the existence of a 0^- state near $E_x = 21.0$ MeV. On the theoretical side, much work has been performed recently to improve the knowledge of ^{4}He near the breakup thresholds (see for example, [1–3]).

The ^{7}Be(n, p)^{7}Li cross section is strongly enhanced near threshold due to a 2^- resonance ($\ell = 0$ in the entrance channel). The cross section at thermal energy is $\sigma_{\text{th}} = 3.84 \times 10^4$ barn [4], which is the largest thermal cross section known in the light element region. This resonance presents quite different proton and neutron widths [16], which is interpreted as an evidence for a strong isospin mixing [17]. According to recent investigations of the ^{7}Li primordial nucleosynthesis, the ^{7}Be(n, p)^{7}Li reaction provides a strong constraint on the different models [5–8]. However, although the cross section is very large, experimental studies [18–22] are made difficult by several reasons: (i) direct measurements require a ^{7}Be radioactive target;

[1] Permanent address: LPHEA, FSSM, Université Caddi Ayyad, Marrakech, Morocco.
[2] Directeur de Recherches FNRS.

(ii) indirect measurements through the ^{7}Li(p, n)^{7}Be reverse reaction not only involve the ^{7}Be ground state, but also a contribution from the first excited state of ^{7}Be, which must be removed to apply the detailed balance theorem.

In the present work, we investigate both (n, p) reactions in the *R*-matrix framework [23]. The *R*-matrix method is known to be well adapted to low-energy reactions [1, 17, 24]. It can be used for resonant as well as for non-resonant reactions. An *R*-matrix analysis has been performed previously for the ^{7}Be(n, p)^{7}Li reaction [22], but the present work extends this calculation by evaluating the uncertainties on the cross section. In addition we also consider an energy range wider than Koehler *et al*, which provides information about some high-lying states of ^{8}Be. Investigations of stellar evolution involve the reaction rate, directly related to the cross section. An evaluation of uncertainties is quite important in big-bang models [5–8], and has received little consideration until now.

In section 2, we present a brief overview of the *R*-matrix framework, with emphasis on transfer reactions. Sections 3 and 4 deal with the analysis of the ^{3}He(n, p)^{3}H and ^{7}Be(n, p)^{7}Li reactions, respectively. In section 5, we compare the reaction rates with previous studies. Concluding remarks are given in section 6.

2. Outline of the *R*-matrix framework

Let us consider two colliding nuclei with masses (A_1, A_2), charges (Z_1e, Z_2e) and spins (I_1, I_2). The transfer cross section from the initial state to a final state is defined as

$$\sigma_t(E) = \frac{\pi}{k^2}\sum_{J\pi}\frac{2J+1}{(2I_1+1)(2I_2+1)}\sum_{\ell\ell' II'}\left|U^{J\pi}_{\ell I,\ell' I'}(E)\right|^2, \tag{1}$$

where E is the c.m. energy in the entrance channel and k the wave number. The collision matrix $\boldsymbol{U}^{J\pi}(E)$ contains the information about the transfer process. In general, for a given total angular momentum J and parity π, several I values (arising from the coupling of I_1 and I_2) and ℓ values are allowed. Quantum numbers (ℓI) and $(\ell' I')$ refer to the entrance and exit channels, respectively. To simplify the procedure, we assume here that a single set of (ℓI) and $(\ell' I')$ values is involved in (1). This is justified at low energies where the lowest angular momentum is strongly dominant.

In this work, the collision matrix is defined in the *R*-matrix formalism, which has been presented in several papers (see, e.g. [23]). Here we briefly describe the procedure for transfer reactions. The *R*-matrix framework assumes that the configuration space is divided into two regions: the internal region (with radius a), where antisymmetrization and nuclear forces are important, and the external region, where the interaction between the nuclei is governed by the Coulomb force only. The physics of the internal region is parametrized by a number N of poles, which are characterized by energy E_λ and reduced width γ_λ. In a multichannel problem, the *R*-matrix at energy E is defined as

$$R_{ij}(E) = \sum_{\lambda=1}^{N}\frac{\tilde{\gamma}_{\lambda,i}\tilde{\gamma}_{\lambda,j}}{E_\lambda - E}, \tag{2}$$

which must be given for each partial wave J. Indices i and j refer to the channels. For the sake of simplicity we do not explicitly write indices $J\pi$ in the *R*-matrix and in its parameters.

Definition (2) can be applied for resonant as well as for non-resonant partial waves. In the latter case, the non-resonant behaviour is simulated by a high-energy pole, referred to as the background contribution, which makes the *R*-matrix almost energy independent. The pole properties $(E_\lambda, \tilde{\gamma}_{\lambda,i})$ are known to be associated with the physical energy and width of resonances, but not strictly equal. This is known as the difference between 'formal' parameters $(E_\lambda, \tilde{\gamma}_{\lambda,i})$ and 'observed' parameters $\left(E^r_\lambda, \gamma_{\lambda,i}\right)$, deduced from experiment. In a general case, involving more than one pole, the link between those two sets is not straightforward [25, 26]. When a single pole is present, the relationship between observed and formal parameters for two-channel reactions is given by

$$\begin{aligned} E^{\mathrm{r}}_1 &= E_1 - \tilde{\gamma}^2_{1,1} S_1\left(E^{\mathrm{r}}_1\right) - \tilde{\gamma}^2_{1,2} S_2\left(E^{\mathrm{r}}_1\right), \\ \gamma^2_{1,i} &= \tilde{\gamma}^2_{1,i} \Big/ \left(1 + \tilde{\gamma}^2_{1,1} S'_1\left(E^{\mathrm{r}}_1\right) + \tilde{\gamma}^2_{1,2} S'_2\left(E^{\mathrm{r}}_1\right)\right), \end{aligned} \tag{3}$$

where $S_i(E)$ are the shift factors, defined from

$$L_i = k_i a \frac{O'_\ell(k_i a)}{O_\ell(k_i a)} = S_i + i P_i. \tag{4}$$

In this expression, O_ℓ is the outgoing Coulomb function, and P_i are the penetration factors, defined in channel i (see [23] for details). For the sake of clarity, index ℓ is not written in the Coulomb functions L, S and P. With equations (3) it is easy to derive the *R*-matrix parameters $\left(E_1, \tilde{\gamma}^2_{1,1}, \tilde{\gamma}^2_{1,2}\right)$ entering equation (2) from the experimental values $\left(E^r_1, \gamma^2_{1,1}, \gamma^2_{1,2}\right)$. As is well known the reduced width is related to the total width $\Gamma_{1,i}$ of the resonance by

$$\Gamma_{1,i} = 2\gamma^2_{1,i} P_i(k_r a), \tag{5}$$

where k_r is the wave number at the resonance energy.

If no resonance is present in the energy range of interest, the *R*-matrix (2) involves high-energy poles only. In that case it can be parametrized by a constant value

$$R_{ij}(E) = R^0_{ij}, \tag{6}$$

with the constraint

$$\left(R^0_{12}\right)^2 = R^0_{11} R^0_{22} \tag{7}$$

if a single pole is involved.

As shown in [24], the collision matrix $\boldsymbol{U}$ is deduced from the *R*-matrix by

$$\begin{aligned} U_{11} &= \frac{I_1}{O_1} \frac{1 - R_{11} L^\star_1 - R_{22} L_2}{1 - R_{11} L_1 - R_{22} L_2}, \\ U_{22} &= \frac{I_2}{O_2} \frac{1 - R_{11} L_1 - R_{22} L^\star_2}{1 - R_{11} L_1 - R_{22} L_2}, \\ U_{12} = U_{21} &= \frac{2\mathrm{i}a\sqrt{k_1 k_2}\sqrt{R_{11} R_{22}}}{O_1 O_2 (1 - R_{11} L_1 - R_{22} L_2)}, \end{aligned} \tag{8}$$

where $I_i = O^\star_i$. The Coulomb functions are evaluated at the channel radius a. Note that, in general, the ℓ values in the entrance and exit channels are different, but here the charge symmetry of both channels yields identical ℓ values.

For the investigation of the ^{3}He(n, p)^{3}H and ^{7}Be(n, p)^{7}Li reactions we select the dominant partial waves, and parametrize them in the *R*-matrix approach. The dominant partial waves correspond to the lowest angular momentum or to resonant states. The reduced widths will be written as γ^2_n for $\gamma^2_{1,1}$ and γ^2_p for $\gamma^2_{1,2}$ since we are dealing with single-pole (n, p) reactions. Each reaction is discussed in more detail in sections 3 and 4.

3. The ^{3}He(n, p)^{3}H reaction

In the low-energy region, the main partial waves correspond to $\ell = 0$ and 1. According to [1], the 0^+_2 ($E_x = 20.21$ MeV), 0^- ($E_x = 21.01$ MeV) and 2^- ($E_x = 21.84$ and 23.33 MeV)

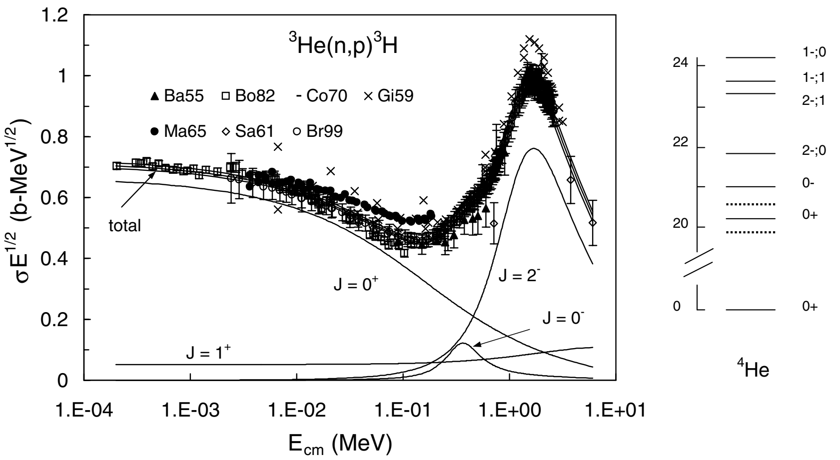

Figure 1. ^{3}He(n, p)^{3}H cross section (multiplied by $\sqrt{E}$), with components of the different partial waves. The data are taken from [9–15], referred to as Ba55, Gi59, Sa61, Ma65, Co70, Bo82 and Br99, respectively. Curves corresponding to 1σ are plotted along with the optimal fit. The spectrum of ^{4}He is given on the right-hand side, with the neutron and proton thresholds displayed as dotted lines.

Table 1. *R*-matrix parameters for the ^{3}He(n, p)^{3}H reaction ($a = 5$ fm). Energies are given in MeV.

J^π	(ℓ, I)	E_r	γ_n^2	γ_p^2	Γ_n	Γ_p
0^+	0, 0	-0.211	2.29	1.02	–	1.16
0^-	1, 1	0.43[a]	1.37	0.05	0.48	0.05
2^-	1, 1	2.61	2.10	1.72	4.53	4.28
J^π	(ℓ, I)	R_{nn}	R_{pp}			
1^+	0, 1	0.16	0.19			

[a] Not fitted.

states (see figure 1) are expected to determine the cross section. They correspond to $(\ell, I) = (0, 0), (1, 1)$ and (1,1), respectively. The role of the two broad 2^- resonances has been simulated by a single pole in the *R*-matrix expansion (2). A $\ell = 0$ non-resonant partial wave, corresponding to $J = 1^+$ has been also taken into account.

The *R*-matrix parameters are given in table 1, and the corresponding cross section (displayed as $\sigma\sqrt{E}$) is shown in figure 1. The χ^2 value is $\chi^2_{\min}/N = 0.36$ ($N = 252$ is the number of data points). The calculations have been performed with $a = 5$ fm. Other choices provide similar energies and widths, with equally good fits of the data. The energy spectrum of ^{4}He near the proton and neutron thresholds is given on the right-hand side of the figure. As mentioned by Borzakov *et al* [15] the cross section near threshold is strongly influenced by the 0^+*s*-wave resonance, which is responsible for the deviation from the $1/v$ law, where v is the relative velocity (a $1/v$ dependence would yield a constant term when $\sigma\sqrt{E}$ is plotted). The γ_n^2 and γ_p^2 values are of the same order of magnitude which confirms a dominant $T = 0$ isospin.

Near $E_{\rm cm} = 0.4$ MeV, the recent data of Brune *et al* [9] suggest a resonance, in agreement with [27]. According to [1], this resonance has been fitted with $J^\pi = 0^-$. Since the data are somewhat uncertain in this energy region, we have fixed the energy of the 0^- state as

Table 2. R-matrix parameters for the $^7Be(n, p)^7Li$ reaction ($a = 5$ fm). Energies are given in MeV.

J^π	(ℓ, I)	E_r	γ_n^2	γ_p^2	Γ_n	Γ_p
2^-	0, 2	0.0027	2.11[a]	0.697[a]	0.225[a]	1.409[a]
3^+	1, 2	0.33[a]	0.253	0.062	0.077	0.088
3^+	1, 2	2.66	0.198	0.199	0.490	0.610
J^π	(ℓ, I)	R_{nn}	R_{pp}			
2^+	1, 2	3.01	2.90			

[a] Not fitted.

$E_{cm} = 0.43$ MeV. The fitted widths ($\Gamma_n = 0.48$ MeV, $\Gamma_p = 0.05$ MeV) indicate a dominant neutron structure, typical of resonances with a strong isospin mixing [17].

Two 2^- resonances are experimentally known [4] at low energies ($T = 0$ at $E_x = 21.84$ MeV, and $T = 1$ at $E_x = 23.33$ MeV). Both resonances are broad (2 MeV and 5 MeV, respectively), and are expected to strongly overlap. Accordingly we have combined both states in a single pole. As shown in figure 1, the maximum observed in the data near $E_{cm} = 2.6$ MeV is well reproduced by the R-matrix fit, but the data are not precise enough to disentangle both 2^- experimental states.

At low energies the collision matrix element U_{11} can be parametrized [28] from the scattering length a_0 and the effective range r_e as

$$U_{11} = \exp(2i\delta_{11}) \qquad k \cot \delta_{11} \approx -\frac{1}{a_0} + \frac{1}{2} r_e k^2, \tag{9}$$

where δ_{11} is the neutron phase shift (complex). These data have not been fitted here; they are used to test the parametrization. For the non-resonant triplet partial wave 1^+, we find $a_0 = (4.25-0.10\,i)$ fm, whereas for the resonant 0^+ partial wave we have $a_0 = (11.9-4.1i)$ fm. The triplet value is in fair agreement with the experiment [29] ($a_t = 3.62 \pm 0.15$ fm); the small imaginary term confirms the weak coupling between the neutron and proton channels. For the singlet scattering length, the experimental value is $a_s = (6.53 \pm 0.32)$ fm $-$ i(4.450 ± 0.003) fm; although we overestimate the real part, the imaginary term, which determines the (n, p) cross section is in nice agreement with experiment.

Uncertainties on the cross section have been evaluated by using standard methods [30]. Cross sections have been generated by many parameter sets around the optimal values (see table 1). Parameter sets corresponding to χ^2 values lower than $\chi^2_{min} + \Delta\chi^2$ have been used to calculate the 1σ uncertainty ($\Delta\chi^2$ depends on the number of parameters [30]). Uncertainties obtained in such a way are typically of the order of 2%.

4. The $^7Be(n, p)^7Li$ reaction

Experimental data are obtained either from direct measurements [22], or from the $^7Li(p, n)^7Be$ reverse reaction [18–21]. The cross section near threshold is strongly enhanced by a 2^- resonance ($\ell = 0$) at $E_x = 18.91$ MeV. In addition, the data show evidence for two peaks; the former corresponds to the (unresolved) 3^+ states at 19.07 and 19.24 MeV, and the latter to the 3^+ resonance at 21.5 MeV.

The R-matrix analysis involves four partial waves, as shown in table 2. The 3^+ states at 19.07 and 19.24 MeV have been replaced by a single resonance, as the data do not enable us to resolve them. This state is not supposed to interfere with the higher 3^+ state at 21.5 MeV. This approximation seems justified since the energy difference is fairly large. To fit the

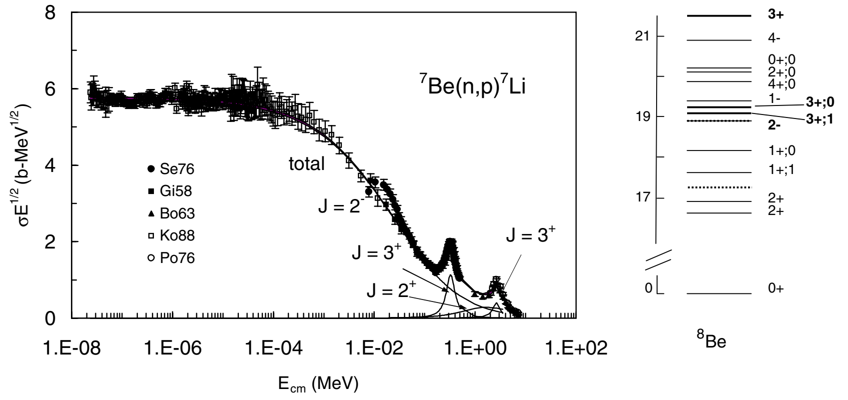

Figure 2. ^{7}Be(n, p)^{7}Li cross section (multiplied by $\sqrt{E}$), with components of the different partial waves. The data are taken from [18–22], referred to as Gi58, Bo63, Po76, Se76 and Ko88, respectively. The thick lines in the level scheme represent the states included in the *R*-matrix analysis.

higher energy part of the data, we found it necessary to include a non-resonant 2^+ ($\ell = 1$) contribution.

The resulting fit is given in figure 2, with individual components of each partial wave. For the 2^- resonance, the data do not allow us to determine the energy and partial widths simultaneously. Accordingly we have taken the neutron and proton widths from the literature [4] and used the energy as a free parameter. As expected, the optimal value is very close to zero. Note that another definition of the width has been used by Koehler *et al* [22]. These authors define the resonance energy and width as the properties of a pole of the *S*-matrix in the so-called Riemann sheet IV [31]. This approach yields a total width much lower than the sum of the proton and neutron partial widths. In our parametrization, the total width is given by $\Gamma = \Gamma_p + \Gamma_n = 1.634$ MeV.

The 3^+ ($T = 1$) and 3^+ ($T = 0$) states at $E_x = 19.07$ and 19.24 MeV are assumed to have different structures [4]: the former essentially decays through proton emission whereas the latter presents a substantial ratio in the neutron channel. Our calculation suggests $\Gamma_n = 77$ keV and $\Gamma_p = 88$ keV, which is not inconsistent with the total width of the 3^+ ($T = 0$) state ($\Gamma = 227 \pm 16$ keV). The 3^+ state at 21.5 MeV is fitted with $\Gamma_n = 0.490$ keV and $\Gamma_p = 0.610$ keV, which corresponds to similar reduced widths. The total width is in good agreement with the experiment ($\Gamma = 1000$ keV).

As for the ^{3}He(n, p)^{3}H reaction, the 1σ uncertainly on the cross section has been determined. Although the error bars are of the order of 5% at low energies, a precise error analysis provides uncertainties less than 1% at the 1σ confidence level. With the optimal parameter, we have $\chi^2_{\min}/N = 0.88 (N = 150)$.

The scattering length for $J = 2^-$ is not known experimentally; our calculation provides $a_0 = (5.0 - 15.1\mathrm{i})$ fm. The large imaginary term reflects the strong absorption in the proton channel.

5. Reaction rates

The ^{3}He(n, p)^{3}H and ^{7}Be(n, p)^{7}Li reaction rates $N_A\langle\sigma v\rangle$ (where N_A is the Avogadro number) are given in figures 3 and 4, respectively. They have been obtained by numerical integration of the theoretical cross sections times the Maxwell–Boltzmann distribution [32].

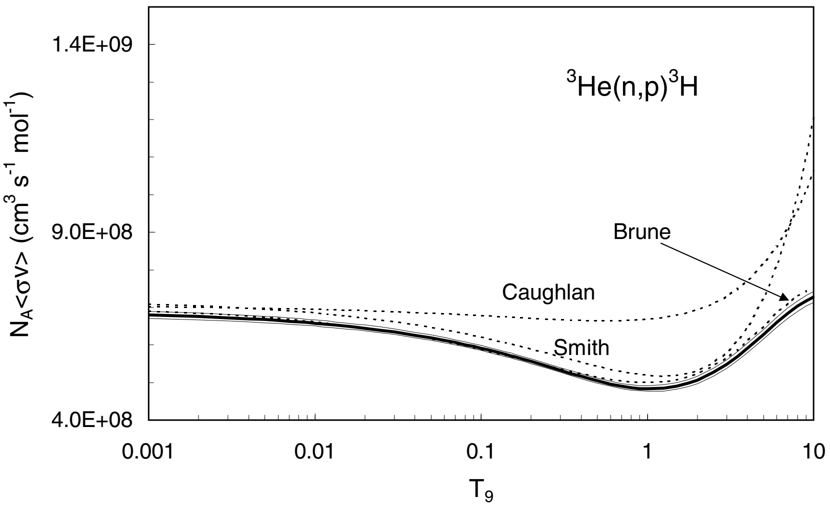

Figure 3. ^{3}He(n, p)^{3}H reaction rates compared with the values of [5, 9, 33].

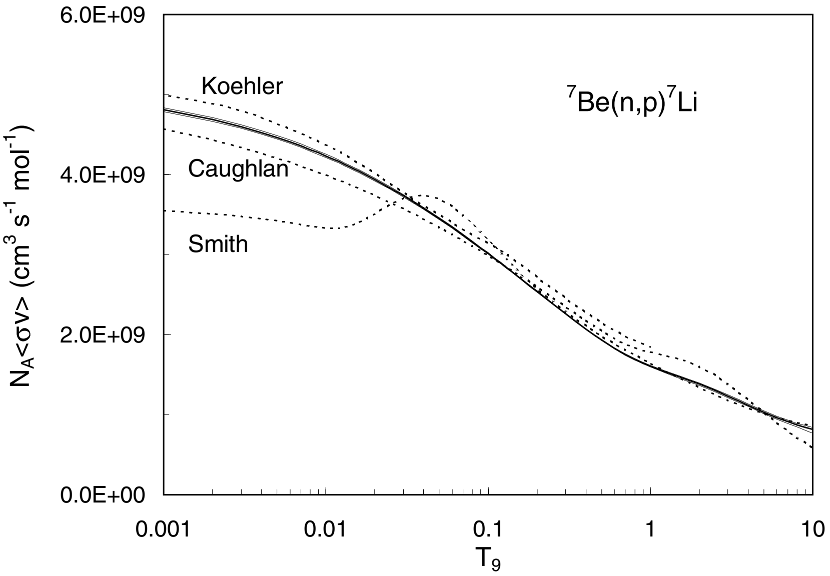

Figure 4. ^{7}Be(n, p)^{7}Li reaction rates compared with the values of [5, 22, 33].

For the ^{3}He(n, p)^{3}H reaction, the 1σ uncertainty is about 2% in a wide temperature range. This is lower than the uncertainty adopted by Smith *et al* [5] (10%). The present uncertainty should allow us to improve the accuracy of big-bang models. The ^{3}He(n, p)^{3}H is one of the key reactions for the production of ^{3}He and ^{7}Li in nucleosynthesis models [5–7]. Our rate essentially agrees with the calculation of Brune *et al* [9], who do not evaluate uncertainties. Up to $T_9 = 3$ the rate determined by Smith *et al* [5] is higher by 5% but is claimed by the authors to be valid up to $T_9 = 6$ only. The Caltech rate [33] agrees with other calculations up to $T_9 \approx 0.01$, but significantly deviates for higher temperatures.

The present ^{7}Be(n, p)^{7}Li reaction rate is between the rates recommended in [33] and [22]. The values obtained by Smith *et al* [5] are significantly smaller at low temperatures ($T_9 \leqslant 0.02$). Beyond $T_9 \approx 0.02$ all rates are in reasonable agreement. According to the cross section presented in figure 2, the uncertainties at the 1σ confidence level are of the order of 1%.

6. Conclusions

In this paper, we have analysed the ^{3}He(n, p)^{3}H and ^{7}Be(n, p)^{7}Li cross sections in the *R*-matrix theory. Both reactions are relevant to nuclear physics and astrophysics. Concerning nuclear physics aspects of our work, we have derived partial widths of low-energy resonances. In the ^{3}He(n, p)^{3}H reaction, the presence of a low-energy 0^- state has been confirmed. For both systems, we have calculated the scattering lengths, which were used as tests of the model.

The main novelty of the present work is the *R*-matrix analysis of the cross section, involving all important partial waves, and complemented by a rigorous determination of the uncertainties on the cross section. At the 1σ confidence level, those uncertainties are lower than previously suggested [5]. Considering all data simultaneously provides uncertainties smaller than the error bar on each data point. For each reaction, the χ^2 values are found fairly small, which indicates the quality of the fits. The present reaction rates, associated with the uncertainty evaluation should help in improving the precision on models of standard big-bang nucleosynthesis.

Acknowledgments

We are grateful to Carl Brune for providing us with the ^{3}He(n, p)^{3}H data in a numerical format. A A thanks the FNRS for financial support. This text presents research results of the Belgian program P5/07 on interuniversity attraction poles initiated by the Belgian-state Federal Services for Scientific, Technical and Cultural Affairs.

References

[1] Tilley D R, Weller H R and Hale G M 1992 *Nucl. Phys.* A **541** 1
[2] Hofmann H M and Hale G M 1997 *Nucl. Phys.* A **613** 69
[3] Csótó A and Hale G M 1997 *Phys. Rev.* C **55** 2366
[4] Ajzenberg-Selove F 1988 *Nucl. Phys.* A **490** 1
[5] Smith M S, Kawano L and Malaney R A 1993 *Astrophys. J. Suppl.* **85** 219
[6] Nollett K M and Burles S 2000 *Phys. Rev.* D **61** 123505
[7] Cyburt R H, Fields B D and Olive K A 2001 *New Astronomy* **6** 215
[8] Coc A, Vangioni-Flam E, Cassé M and Rabiet M 2002 *Phys. Rev.* D **65** 043510
[9] Brune C R, Hahn K I, Kavanagh R W and Wrean P R 1999 *Phys. Rev.* C **60** 015801
[10] Batchelor R, Aves R and Skyrme T H R 1955 *Rev. Sci. Instrum.* **26** 1037
[11] Gibbons J H and Macklin R L 1959 *Phys. Rev.* **114** 571
[12] Sayres A R, Jones K W and Wu C S 1961 *Phys. Rev.* **122** 1853
[13] Macklin R L and Gibbons J H 1965 Nuclear structure study with neutrons *Proc. Int. Conf. on the Study of Nuclear Structure with Neutrons (Antwerp)* ed M Nève de Mévergnies, P Van Assche and J Vervier (Amsterdam: North-Holland 1966) p 498
Macklin R L and Gibbons J H 1965 *Oak Ridge National Laboratory Report* No ORNL-P-1375
[14] Costello D G, Friesenhahn S J and Lopez W M 1970 *Nucl. Sci. Eng.* **39** 409
[15] Borzakov S B, Malecki H, Pikel'ner L B, Stempinski M and Sharapov É I 1982 *Yad. Fiz.* **35** 532
Borzakov S B, Malecki H, Pikel'ner L B, Stempinski M and Sharapov É I 1982 *Sov. J. Nucl. Phys.* **35** 307
[16] Newson H W, Williamson R M, Jones K W, Gibbons J H and Marshak H 1957 *Phys. Rev.* **108** 1294
[17] Barker F C 1977 *Aust. J. Phys.* **30** 113
[18] Macklin R L and Gibbons J H 1958 *Phys. Rev.* **109** 105

[19] Borghers R R and Poppe C H 1963 *Phys. Rev.* **129** 2679
[20] Poppe C H, Anderson J D, Davis J C, Grimes S M and Wong C 1976 *Phys.Rev.* C **14** 438
[21] Sekharan K K, Laumer H, Kern B D and Gabbard F 1976 *Nucl. Instrum. Methods* **133** 253
[22] Koehler P E, Bowman C D, Steinkruger F J, Moody, Haight R C, Lisowski P W and Talbert W L 1988 *Phys. Rev.* C **37** 917
[23] Lane A M and Thomas R G 1958 *Rev. Mod. Phys.* **30** 257
[24] Angulo C and Descouvemont P 1998 *Nucl. Phys.* A **639** 733
[25] Angulo C and Descouvemont P 2000 *Phys. Rev.* C **61** 064611
[26] Brune C R 2002 *Phys. Rev.* C **66** 044611
[27] Walston J R, Keith C D, Gould C R, Haase D G, Raichle B W, Seely M L, Tornow W, Wilburn W S, Hoffmann G W and Penttilä S I 1998 *Phys. Rev.* C **58** 1314
[28] Preston M A and Bhaduri R K 1975 *Structure of the Nucleus* (Reading, MA: Addison-Wiley)
[29] Alfimenkov V P, Borzakov S B, Van Tkhuan Vo, Govorov A M, Lason L, Pikelner L B and Sharapov E I 1981 *Yad. Fiz.* **33** 891
[30] Hagiwara K *et al* 2002 *Phys. Rev.* D **66** 010001
[31] Frazer W R and Hendry W A 1964 *Phys. Rev.* **134** B1307
[32] Clayton D D 1983 *Principles of Stellar Evolution Nucleosynthesis* (Chicago, IL: University of Chicago Press)
[33] Caughlan G R and Fowler W A 1988 *At. Data. Nucl. Data Tables* **40** 283